Structural fluctuations and the order-disorder phase transition in calcite

1994 J. Phys.: Condens. Matter 6 1345

(http://iopscience.iop.org/0953-8984/6/7/007)

J. Phys.: Condens. Matter 6 (1994) 1345–1358. Printed in the UK

Structural fluctuations and the order–disorder phase transition in calcite

M Ferrario†, R M Lynden-Bell‡ and I R McDonald‡

† Dipartimento di Fisica, Università di Messina, Casella Postale 50, 98166 S Agata-Messina, Italy

‡ University Chemical Laboratory, Lensfield Road, Cambridge CB2 1EW, UK

Received 29 September 1993, in final form 1 December 1993

Abstract. Molecular-dynamics calculations have been carried out on the ordered (low-temperature) and orientationally disordered (high-temperature) phases of calcite. The potential model used is shown to reproduce the main features of the experimentally observed order–disorder transition. The significance of the results for the interpretation of recent inelastic neutron-scattering experiments is discussed with particular reference to a possible competition between different ordering processes. Comparison is made with previously reported simulations of the corresponding phase transition in sodium nitrate and differences in behaviour between the two systems are noted.

1. Introduction

In an earlier paper [1], to be referred to as I, we reported the results of a series of molecular-dynamics computer simulations of the ordered low-temperature and orientationally disordered high-temperature phases of crystalline sodium nitrate. The phase transition is of second order [2] and is similar to the transition between ordered and disordered phases in the calcite form of calcium carbonate [3]. The transition temperature is much higher for calcite (1260 K) than for sodium nitrate (549 K); this makes the transition in calcite more difficult to study experimentally, since calcium carbonate readily decomposes ($CaCO_3 \rightarrow CaO+CO_2$) at temperatures above about 1200 K. All the evidence suggests [2–4], however, that the structural changes are very similar in the two cases. In both the ordered and disordered phases the molecular anions are stacked in planes perpendicular to the [001] direction, i.e. with their threefold axes lying along the c-axis of the crystal. Below the transition, the space group is $R\bar{3}c$; all molecules in a given plane have the same orientation with respect to the a and b axes, which differs by 60° from that of anions in adjacent planes. (Throughout this paper we follow the convention adopted in I whereby all crystallographic information is presented in terms of the $R\bar{3}c$ structure in its hexagonal setting.) Above the transition, the anions are disordered with respect to 60° rotations about their threefold axes, and the symmetry is $R\bar{3}m$. Heating the crystal through the phase transition therefore leads to a halving of the unit cell in the c-direction and a consequent reduction in the number of Bragg points. The onset of orientational disorder is also accompanied by an unusually rapid increase with temperature of the unit-cell parameter c, while the parameter a shows a small *decrease*.

A key aspect of the order–disorder transition in both materials is the fact that the difference in structure of the two phases is associated solely with the orientational ordering

0953-8984/94/071345+14$19.50

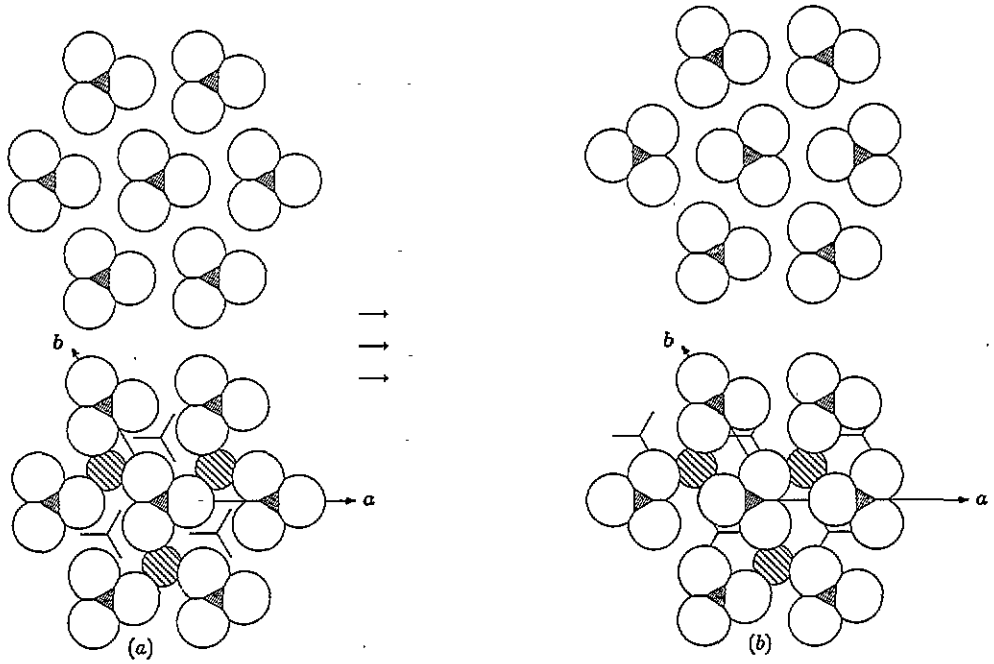

Figure 1. Section through the reciprocal lattice of the $R\bar{3}m$ structure in the convention of Dove *et al* [8]. The plane shown corresponds to $b^* = 0$ and selected lattice points are labelled. Large filled circles are Bragg points in both the ordered and disordered phases of calcite; small filled circles are Z points, which are Bragg points in the experimentally observed low-temperature structure (Z phase); small open circles are F points, which would be Bragg points in the postulated F^{1-} phase; and the large open circle is the Γ point. The bold continuous line is line 1 of the text; the bold dashed line is the projection of line 2 of the text onto the plane shown. The two F points on line 1 are $(2.5, 0, 2) \equiv F_a$ and $(3.5, 0, -2) \equiv F_b$.

of the anions. Figure 1 shows a cross-section through the reciprocal lattice of the high-temperature phase with the zone centre Γ and the special points Z and F (see below) marked. The low-temperature structure is related to the structure at high temperatures by ordering at the Z points. The Z points therefore become Bragg points below the transition; because the centre-of-mass structure has the same symmetry ($R\bar{3}m$) in each phase, the additional reflections seen in x-ray- or neutron-diffraction experiments on the ordered form arise solely from the scattering by oxygen atoms. The intensities of these Bragg reflections are proportional to the square of the macroscopic order parameter, Q, for the transition, which is found [2, 3] to vary with temperature in the form typical of a second-order transition, i.e.

$$Q \propto |T_c - T|^{\beta} \tag{1}$$

where T_c is the critical temperature and β is a critical exponent; the choice of an appropriate microscopic representation of Q is discussed below. Experiments show that $\beta = 0.25$ over a wide range of temperature, which is the value expected for a classical tricritical transition. One feature of the order–disorder transition which is different in sodium nitrate and calcite is that while in calcite β remains equal to 0.25 as the transition is approached, in sodium

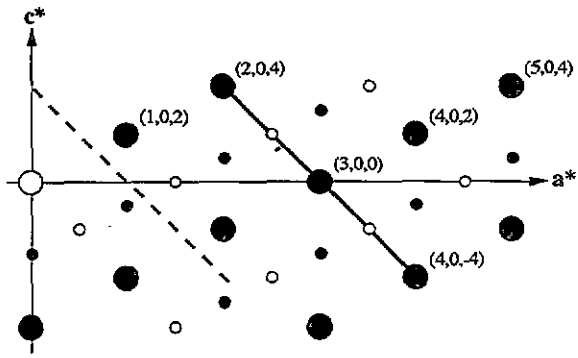

Figure 2. (*a*) Structure of the ordered ($R\bar{3}c$) phase of calcite. The upper part of the figure shows a plane of carbonate ions, while in the lower part of the figure the cations in the layer below that plane are shaded and the positions and orientations of the carbonate ions in the layer below that are indicated by bond vectors. (*b*) View of the hypothetical F^{1-} phase. Carbonate ions in the central row are rotated by 180° with respect to the $R\bar{3}c$ structure and the rows indicated by arrows are shifted by 1 Å to the left.

nitrate [2] it changes to a value of 0.22 at a temperature approximately 30 K below T_c. Local fluctuations in structure can also be expected to give rise to strong diffuse scattering close to the Z points; this is true of both the high- and low-temperature phases.

In the calculations for sodium nitrate reported in I we found evidence for an alternative ordering scheme involving an instability at the F point (see figure 1) rather than the Z point of the high-temperature structure. A variety of experimental observations has been reported of anomalies near the F points in the disordered phase [5–7] and it has also been suggested [2] that a competition between ordering schemes could provide a natural explanation for the reduction in β below its classical value. The real-space structure of the hypothetical F^{1-} phase proposed in I is illustrated in figure 2; the symmetry label F^{1-} indicates that the reciprocal lattice is antisymmetric with respect to reflection through a plane containing c^* and the wavevector corresponding to the F point. The structure is monoclinic, space group $P2/a$, and differs from the observed $R\bar{3}c$ structure, or Z phase, by both centre-of-mass translations and rotations of anions in alternate planes. Hence any contribution to the diffuse scattering from fluctuations of F^{1-}-type order will include contributions from all atoms, not merely from the oxygens, though since the oxygen atoms are three times more numerous than carbon or sodium, scattering from oxygens will be the dominant contribution. Confirmation of whether or not the model of structural fluctuations proposed in I is appropriate to real sodium nitrate is still awaited. The only direct evidence in favour of the postulated competitive ordering process is the unusually strong diffuse x-ray scattering observed at certain points in reciprocal space by Shinnaka [5]. Recently, however, Dove *et al* [8] have suggested that anomalies seen in the results of inelastic neutron-scattering experiments on calcite can be explained in a similar way. In the present paper, therefore, we apply the methods developed in I to the case of calcite. We address the questions of whether there is evidence for F^{1-}-point as well as Z-point ordering in calcite and of how far the effects reported by Dove *et al* [8] can be interpreted in terms of incipient F-point ordering of the type in question.

In seeking evidence of F-point ordering in either the experiments or the simulations there is an important symmetry consideration to be borne in mind. The character table

of the space group $R\bar{3}m$ shows that there are four symmetry species associated with the F point [9]; these are labelled F^{1+}, F^{2+}, F^{1-} and F^{2-}, respectively. The structure of the proposed F phase has F^{1-} symmetry. Of the three translational phonons (acoustic or optic) at the F point, the two 'in-plane' vibrations transform as F^{2-} and the one 'out-of-plane' vibration transforms as F^{1-}. Only the latter symmetry species is involved directly in the postulated F ordering. Thus, in order to observe fluctuations of the relevant symmetry, the neutron or x-ray response functions must be measured or calculated for q-vectors having an out-of-plane component.

2. Molecular-dynamics calculations

2.1. The model

The potential model used in the simulations is that developed by Dove *et al* [10] by fitting to the structures and elastic constants of both calcite and aragonite and the phonon frequencies of calcite. The interionic ingredients of the model are (i) Coulomb interactions between charges q_{Ca}, q_C and q_O on calcium, carbon and oxygen atoms, respectively and (ii) Born–Mayer repulsive potentials of the form

$$V(R) = A\exp(-R/\rho) \tag{2}$$

for Ca...O and O...O. The original model also included bond-stretching, bond-bending and torsional terms to describe the distortion of the carbonate group, but for simplicity and computational economy we have ignored these terms and treated the anions as rigid, planar objects with a C–O bond length of 1.284 Å. A full list of parameter values is given in [10]. Note that in the model the calcium ion carries a charge less than $2e$ ($q_{Ca} = 1.642e$, with $q_C + 3q_O = -1.642e$); this is in contrast to the fully ionic model developed for sodium nitrate in I ($q_{Na} = e$, $q_N = 0.95e$, $q_O = -0.65e$).

2.2. Technical details of the simulations

The molecular-dynamics calculations were carried out by the same standard methods [11] used in I. The equations of motion were integrated by means of the Verlet algorithm, with a time step of 0.005 ps, while the rigid-body rotational motion of the anions was handled by the generalized method of constraints. The production runs were typically 5000 time steps in length. The normal periodic boundary conditions were used and the Coulomb interactions were treated by the Ewald method. The pair potentials, including the real-space term in the Ewald potential, were truncated at site–site separations of 16.8 Å. The rapidly varying form of the Born–Mayer interaction and the neglect of any contribution from dispersion forces means that the long-range corrections, computed in the usual way, are negligibly small. From that point of view, the chosen truncation separation is unnecessarily large, but the value used was chosen in order to achieve virtually complete convergence of the Ewald sum, particularly of the contribution to the component of the stress tensor corresponding to expansion along the c-axis. A series of preliminary studies showed that less accurate treatments of the Ewald sum gave rise to significant errors in this quantity. Any such error is undesirable, given the experimentally established correlation between thermal expansion and orientational disordering of the anions. The requirement of having a large cut-off in the potential also prompted the decision to use a much larger system than in the work reported in I. All calculations discussed here were based on use of a periodic cell of dimensions $8a \times 8b \times 2c$, i.e. 128 hexagonal unit cells or $N = 768$ molecules. For comparison, the largest system size used in I contained $N = 192$ molecules ($4a \times 4b \times 2c$), and most of the calculations were made for $N = 108$ ($3a \times 3b \times 2c$).

Table 1. Results of zero-pressure calculations at $T = 300$ K.

	a (Å)	c (Å)
Calculated[a]	4.9843	17.478
Fitted[b]	4.9822	17.326
Observed[c]	4.9894	17.039

[a] Results of simulations; statistical uncertainties are ±0.0005 Å in a and ±0.001 Å in c.
[b] Results of fitting procedure used by Dove *et al* [8]; see text for details.
[c] Experimental results from [2].

2.3. Summary of the molecular-dynamics runs

In the first stage of the work, a series of runs designed to test the adequacy of the potential model were carried out under conditions of constant temperature and pressure ($p = 0$) by the Rahman–Parrinello method [11], in which all cell lengths and cell angles are allowed to fluctuate. Table 1 shows the results obtained at $T = 300$ K and allows comparison to be made with the calculations of Dove *et al* [10], who derived their potential parameters by fitting to experimental data corresponding to the same temperature. However, since the fitting procedure used is based on energy minimization, it takes no account of thermal effects. Not surprisingly, therefore, the cell lengths obtained in the simulation are slightly larger than those calculated by Dove *et al* [10]. Although the differences are sufficiently small to justify the fitting procedure, better agreement could be expected for a potential obtained by fitting to the lattice parameters corresponding to zero absolute temperature. Insofar as comparison with experiment is concerned, the main discrepancy is in the value of the lattice parameter c [3], an immediate consequence of which is the fact that the mean volume per formula unit in the simulation (62.67 Å^3) is approximately 2% larger than the experimental result (61.22 Å^3). Hexagonal symmetry was well preserved throughout the molecular-dynamics run; fluctuations in the cell angles about their ideal values were typically ±0.1°.

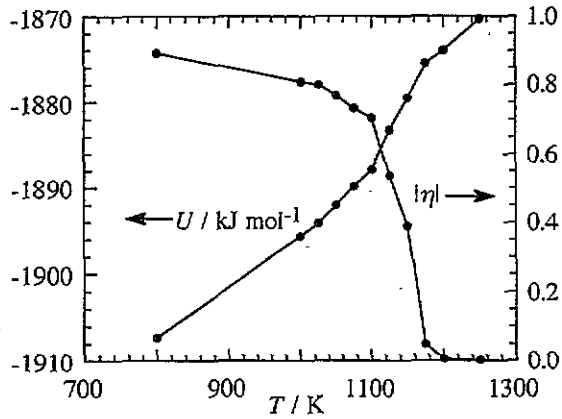

Figure 3. Temperature dependence of the potential energy U and order parameter η. The results were obtained from simulations at constant pressure.

Constant-pressure calculations were then carried out for temperatures between 800 and 1250 K, the primary purpose of which was to determine whether or not the model was able to

reproduce the experimentally observed order–disorder transition. The onset of orientational disorder of the anions was monitored by observing the temperature variation of the single-ion order parameter defined as

$$\eta = \langle (-1)^L \cos(3\phi_i) \rangle \tag{3}$$

where ϕ_i is the angle between the a-axis of the crystal and a randomly chosen C–O bond of the ith carbonate ion, L numbers successive layers of anions perpendicular to the c-axis, and the angular brackets denote a double average over time and over anions i. The quantity η is equal to unity in the ordered phase; it is unaffected by motion ($\pm 120°$) between equivalent orientations, but falls to zero if the ions undergo random $\pm 60°$ reorientations of the type that characterize the transition to the disordered phase. The results obtained for the order parameter η and the interionic potential energy U are plotted as functions of temperature in figure 3. The rapid decrease in η above 1100 K shows that a disordering transition has occurred; the transition is probably complete at 1175 K and is certainly so at 1200 K. Thus not only does the anticipated phase change take place, but the transition temperature is no more than 6–8% different from the value observed experimentally. This is a remarkably good level of agreement, given that the parameters of the interaction model were derived without reference to any property of the disordered phase. Extrapolation of the energies in the regions above and below the transition show that the disordering process involves an energy increase of roughly 7 kJ mol^{-1}. This is very close to the value calculated [10] from the same potential model, but inclusive of intraionic terms, for the energy difference between the ideal Z and F^{1-} structures, namely 0.072 eV per formula unit or 6.9 kJ mol^{-1}. Figure 4 shows the temperature dependence of the unit-cell parameters a and c. As expected, the parameter c increases rapidly with temperature, particularly just below the transition; in the ordered phase, a shows a small increase rather than the small decrease observed experimentally, but at the transition there is an abrupt decrease of approximately 0.005 Å. The effects observed are relatively larger than in sodium nitrate, but this is not surprising, since the electrostatic interactions are stronger. In the ordered phase (figure 2), the nearest neighbours of each calcium ion are three oxygen atoms from different carbonate ions in the plane above and three in the plane below; the orientations of the two triangles of oxygen atoms are staggered with respect to each other. As the anions disorder, the arrangement of oxygen atoms around each calcium ion becomes electrostatically less favourable, and the planes are pushed apart. This, in turn, allows the carbonate ions to tip out of the planes in which they lie initially, causing the lattice parameter a to shrink.

Table 2. Results of constant-volume calculations. Statistical uncertainties are ± 0.2 kJ mol^{-1} in U, ± 0.05 kbar in p and ± 0.01 in η.

	T (K)		
	800	1125	1200
a (Å)	4.9822	5.0080	5.0044
c (Å)	18.319	18.340	18.628
$-U$ (kJ mol^{-1})	1907.5	1885.1	1874.6
p (kbar)	0.19	−0.29	0.05
$\lvert\eta\rvert$	0.89	0.60	0.01

Finally, the runs at $T = 800$, 1125 and 1200 K were repeated under constant-volume conditions with hexagonal symmetry imposed and the parameters a and c fixed at the values

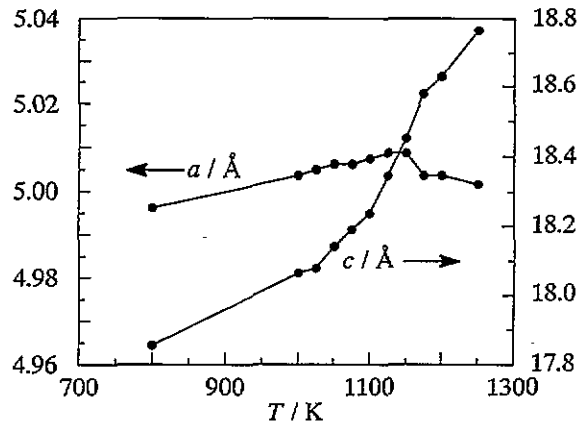

Figure 4. Temperature dependence of the unit-cell parameters a and c. Note the difference between the two vertical scales. The results were obtained from simulations at constant pressure.

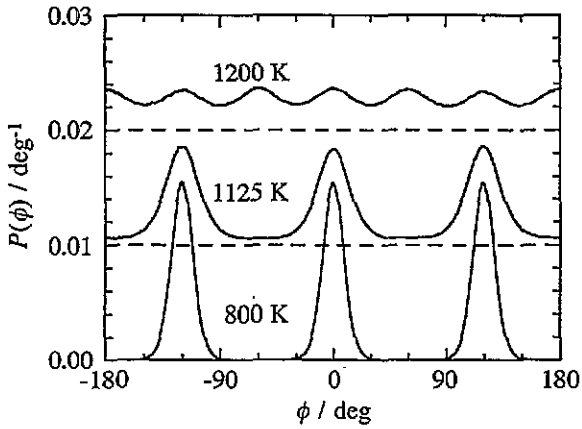

Figure 5. Probability distribution function $P(\phi)$ at three temperatures for the angle ϕ involved in the definition (3) of the orientational order parameter η for the carbonate ions. Note the change from three to six peaks between $T = 1125$ K and $T = 1200$ K. The curves for 1125 and 1200 K have been shifted upwards by 0.01 and 0.02, respectively; the broken lines are the origins for these curves.

obtained in the constant-pressure calculations. These temperatures were chosen as typifying the system in almost completely ordered, partially disordered and fully disordered states, respectively; the assumed values of a and c, together with the calculated energies, pressure and order parameters, are listed in table 2. The section that follows is concerned with a detailed analysis of the results on collective properties obtained in the three constant-volume runs. As a preliminary to that discussion, we show in figure 5 the calculated single-ion probability distributions, $P(\phi)$, for the angle ϕ involved in the definition (3) of the order parameter η; the figure provides a particularly clear illustration of the nature of the disordering transition. At 800 K, reorientational motion of the anions consists solely of librations about the equilibrium sites of the $R\bar{3}c$ structure. At 1125 K, there is evidence of molecules moving between equivalent sites, but the distribution retains

the three-peak form characteristic of the ordered phase. Between 1125 and 1200 K, however, there is an evolution from a three-site distribution of orientations to a continuous distribution with six preferred sites, signalling the appearance of $\pm 60°$ reorientations around the molecular threefold axes. The conclusion that the motion remains primarily librational up to temperatures very close to the transition is in agreement with recent neutron-diffraction studies of calcite by Dove *et al* [12], who have obtained estimates of the mean-square librational amplitude, $\langle \phi^2 \rangle$, at temperatures between 300 and 1150 K. If fluctuations around equilibrium are sufficiently small, the right-hand side of equation (3) may be expanded to give

$$\eta \simeq 1 - 9\langle \phi^2 \rangle / 2. \tag{4}$$

Taking the values of η in table 2, we find $\sqrt{\langle \phi^2 \rangle} \simeq 9°$ at 800 K and $\sqrt{\langle \phi^2 \rangle} \simeq 17°$ at 1125 K. The results reported by Dove *et al* [12] are $\sqrt{\langle \phi^2 \rangle} \simeq 8°$ at 800 K and $\sqrt{\langle \phi^2 \rangle} \simeq 16°$ at 1125 K. The excellence of the agreement between simulation and experiment is partly fortuitous: at least in the case of the simulation at 1125 K, it is certainly not correct to treat the motion as purely librational (see figure 5). In addition, the transition temperature in real calcite is higher than the simulations predict. Nonetheless, the agreement achieved, taken together with the results of figures 3 and 4, is good enough to be able to conclude that the model used in the simulations captures the essential features of the experimentally observed transition.

3. Results and discussion

3.1. Choice of q-vectors

In analyzing the ionic trajectories computed in the constant-volume runs, the main computational effort has been directed at the calculation of quantities relevant to the recent inelastic neutron-scattering studies of calcite made by Dove and coworkers [8, 14]. Calculations have been made along two lines in q-space, as illustrated in figure 1. Line 1 corresponds to $q = (\zeta, 0, 12-4\zeta)$ with $\zeta = 2$–4. This is the range investigated by Dove *et al* [8]. The line runs between Bragg points (2, 0, 4 and 4, 0, −4), passing through an F point, which we shall call F_a at (2.5, 0, 2), another Bragg point at (3, 0, 0), and a second F point (F_b) at (3.5, 0, −2). Note that since the q-vectors along this line lie in the plane of figure 1, only in-plane fluctuations are probed. Line 2 corresponds to $q = (\zeta - 2, 1, 12-4\zeta)$, with $\zeta = 2$–4, and is parallel to line 1 but displaced by the Bragg vector (−2, 1, 0). It again includes three Bragg points, those at $(0, 1, 4)(\zeta = 2)$, $(1, 1, 0)(\zeta = 3)$ and $(2, 1, -4)(\zeta = 4)$, and two F points, at $F_c \equiv (0.5, 1, 2)(\zeta = 2.5)$ and $F_d \equiv (1.5, 1-2)(\zeta = 3.5)$, but in contrast to line 2 the q-vectors now have a component along b^*, thereby allowing both in-plane and out-of-plane fluctuations to be probed. Hence fluctuations of the F^{1-} structure will show themselves at F_c and F_d, but not at F_a and F_b.

The static neutron response function

$$S(q) = \langle \rho^*(q)\rho(q) \rangle \tag{5}$$

and the intermediate scattering function

$$F(q, t) = \langle \rho^*(q, 0)\rho(q, t) \rangle \tag{6}$$

were calculated along lines 1 and 2 from the fluctuations in the neutron-weighted atomic densities defined as

$$\rho(q, t) = (1/\sqrt{N_a}) \sum_i b_i \exp[-iq \cdot r_i(t)] \tag{7}$$

where $r_i(t)$ denotes the coordinates of atom i at time t, $N_a(= 5N)$ is the total number of atoms, and b_i is the coherent neutron scattering length of the ith nucleus; the scattering lengths were taken as 0.490 for calcium, 0.663 for carbon and 0.575 for oxygen, all in units of 10^{-14} m. The dynamic response function $S(q, \omega)$ measured by inelastic neutron scattering [8] is then obtained by calculating numerically the Fourier transform of $F(q, t)$ with respect to t.

3.2. Diffuse scattering

Away from the Bragg points, the only contribution to $S(q)$ is from diffuse scattering. At the Bragg points themselves, however, Bragg scattering is dominant. It can therefore be anticipated that incipient ordering into a different structure will be signalled by anomalously strong diffuse scattering at points in q-space that correspond to Bragg points of the alternative structure but not of the existing one. In particular, fluctuations of F^{1-}-type order should be accompanied by strong scattering at certain of the F points of the $R\bar{3}m$ structure.

The calculated values of $S(q)$ as functions of ζ along lines 1 and 2 (except at the Bragg points) for $T = 800$, 1125 and 1200 K are shown in figure 6. The behaviour is simpler along line 2, for which there is a significant degree of scattering at all accessible q-values. (The term accessible refers here to q-values compatible with the periodic boundary conditions used in the simulations: the plotted curves include all such points along the chosen lines.) Not surprisingly, the intensity of the diffuse scattering increases as the temperature is raised and the system becomes more disordered. On the other hand, there are no special features associated with the F points. The intensities there are not appreciably greater than at other points along the line—indeed the point F_d lies close to a local minimum in $S(q)$—and the temperature dependence is not unusually strong: there is nothing here that has not been seen in similar calculations for other disordered crystals. The variation in $S(q)$ along line 1 is less easy to understand. First, there are several q-values at which the intensity of the diffuse scattering decreases with temperature, contrary to what intuition would suggest. Note, in particular, the complete reversal in behaviour relative to line 2 close to the Bragg points at $\zeta = 3.0$ and $\zeta = 4.0$. Secondly, the intensity is a maximum at the point F_a and increases more rapidly with temperature there than at any other point. By contrast, the intensity at the point F_b is relatively weak and scarcely alters with temperature.

The results of figure 6 are not suggestive of any significant degree of F^{1-}-ordering. Such fluctuations would be expected to show up predominantly in the diffuse scattering near F_c and F_d, which correspond to q-values having an out-of-plane component. The fluctuations that do occur are concentrated near F_a, and therefore lack the symmetry appropriate to the postulated F^{1-} phase. It is possible that the in-plane motions probed at the point F_a are coupled by higher-order effects to the out-of-plane fluctuations characteristic of F-point ordering. If that were the case, however, it seems implausible that the out-of-plane fluctuations would not also manifest themselves at F_c and F_d. It is more likely that the enhanced diffuse scattering at F_a is due to low-frequency phonons. Note that the lattice-dynamics calculations of Dove *et al* [10] reveal the presence of a local minimum in the frequency of the in-plane transverse acoustic phonon at the F point, where its symmetry is F^{2-}.

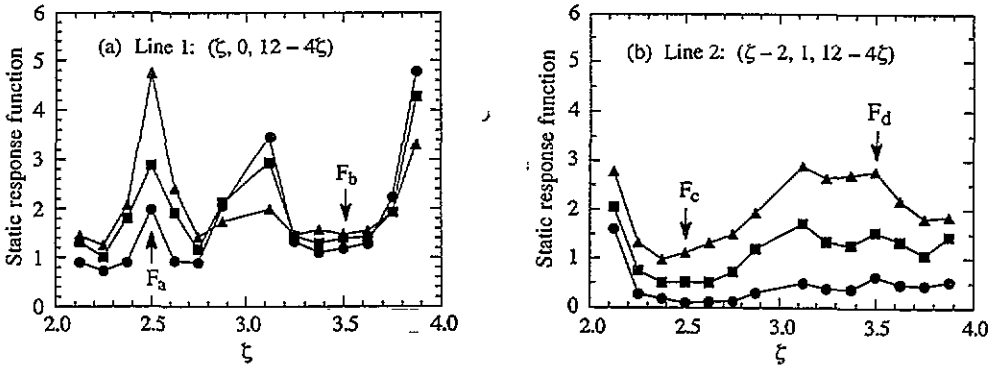

Figure 6. Wavevector dependence of the static response function $S(q)$ (in units of 10^{-28} m^2 per formula unit) along (*a*) line 1 and (*b*) line 2 in reciprocal space (see figure 1). Circles, $T = 800$ K; squares, $T = 1125$ K; triangles, $T = 1200$ K.

3.3. Orientational order and translation–rotation coupling

Support for the conclusions contained in section 3.2 comes from a study of the static translation–rotation coupling. As in I, the amplitudes of fluctuations in orientational order at different points in the first Brillouin zone were measured by calculation of the mean-square values of the collective orientational variables $Y(\boldsymbol{k})$ defined as

$$Y(\boldsymbol{k}) = (1/N)\sum_i \cos(3\phi_i)\exp(-i\boldsymbol{k}\cdot\boldsymbol{R}_i^0) \tag{8}$$

where the sum on i runs over the anions, ϕ_i has the same meaning as in (3) and $\boldsymbol{R}_i^0 \equiv (X_i^0, Y_i^0, Z_i^0)$ denotes the equilibrium centre-of-mass coordinates of an ion; the z direction is taken parallel to the c-axis of the crystal. The ensemble averages of $Y(\boldsymbol{k})$ yield a set of generalized order parameters, $Q(\boldsymbol{k}) \equiv \langle Y(\boldsymbol{k})\rangle$, of which $Q(\boldsymbol{k})_z$ is equivalent to the order parameter η of (3), where $\boldsymbol{k}_Z$ is the wavevector corresponding to the Z point. In the fully disordered phase all $Q(\boldsymbol{k})$ are zero and in the ideal $R\bar{3}c$ structure $Q(\boldsymbol{k}_Z)$ is unity. The extent of translation–rotation coupling at a point $\boldsymbol{k}$ is measured by the correlation coefficient

$$\Xi(\boldsymbol{k}) = \langle s^*(\boldsymbol{k})Y(\boldsymbol{k})\rangle / (\langle s^*(\boldsymbol{k})s(\boldsymbol{k})\rangle\langle Y^*(\boldsymbol{k})Y(\boldsymbol{k})\rangle)^{1/2} \tag{9}$$

where, as discussed in I, $s(\boldsymbol{k})$ is the collective translational variable corresponding to the out-of-plane transverse acoustic phonon, i.e.

$$s(\boldsymbol{k}) = (1/\sqrt{N})\sum_i (Y_i = Y_i^0)\exp(-i\boldsymbol{k}\cdot\boldsymbol{R}_i^0) \tag{10}$$

where the sum on i now runs over all ions and $Y_i(t)$ is the y-coordinate of the centre of mass of ion i at time t. For a mixed order–disorder displacive phase transition which involves translation–rotation coupling, $|\Xi|^2$ tends to unity as the transition temperature is approached from above and the fluctuations become more strongly correlated. The work described in I (for sodium nitrate) and in [13] (for sodium cyanide) shows that the value of $|\Xi|^2$ provides a useful measure of the strength of precursor effects in simulations of disordered crystals. In the case of sodium nitrate [1], regions were found near the Z and

F points where orientational fluctuations were unusually large. The behaviour seen here is different. Fluctuations are again strong near the Z points, but although there are maxima near the F points, they are weaker and broader than in the case of sodium nitrate. In sodium nitrate the quantity $|\Xi|^2$ was shown to reach very high values at the F points (up to 0.93 in a simulation of a partially ordered crystal), suggesting that the system was close to undergoing a transition to the F^{1-} phase. Here the maximum values of $|\Xi|^2$ is appreciably smaller (0.66 at 1125 K and 0.78 at 1200 K). Previously we concluded that F^{1-} ordering is a serious competitor to Z ordering in sodium nitrate, and speculated that this could be the origin of the experimentally observed reduction below its classical value (from 0.25 to 0.22) of the critical exponent β. It appears from our present calculations that, at least for the potential model we have used, F^{1-} ordering is less important in calcite; this is not inconsistent with the fact that experimentally β is larger than for sodium nitrate.

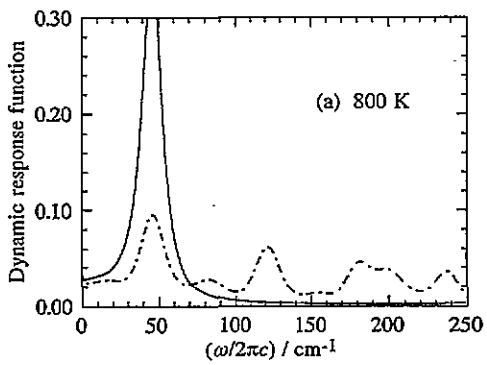

Figure 7. Dynamic response function $S(q, \omega)$ (in arbitrary units) at the points F_a and F_b and temperatures of (*a*) 800 K and (*b*) 1125 K. Continuous lines, F_a; broken lines, F_b.

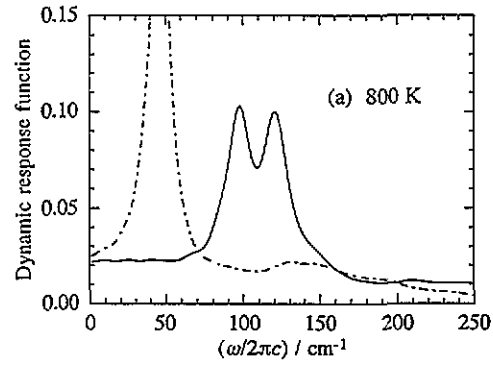

Figure 8. Dynamic response function $S(q, \omega)$ (in arbitrary units) at the reciprocal-lattice points F_c and F_d and temperatures of (*a*) 800 K and (*b*) 1125 K. Continuous lines, F_c; broken lines, F_d.

3.4. Dynamic response function

Figures 7 and 8 shows the response functions $S(q, \omega)$ calculated from the simulations at 800 K and 1125 K for each of the four F points discussed in section 1. At 800 K, which is well below the order–disorder transition, phonon peaks are clearly visible. Separate

calculations of the pure phonon response functions (one-phonon approximation) in the manner described in I show that at 800 K the in-plane (F^{2-}) acoustic phonons occur at frequencies of 48 and 122 cm^{-1} while the out-of-plane phonon (F^{1-}) is at 97 cm^{-1}; the optic response functions have peaks at 145, 195 and 240 cm^{-1} (in-plane) and at 130, 190, 240 and 270 cm^{-1} (out-of-plane). The spectrum at F_a (figure 7) shows only the lowest-frequency (48 cm^{-1}), transverse acoustic mode, while that at F_b has peaks corresponding not only to the F^{2-} acoustic phonons but also to higher-frequency optic and librational modes; the modes are strongly mixed. It should be recalled from section 1 that both F_a and F_b probe the in-plane but not the out-of-plane motions. The differences between spectra at these two points reflect the change in q-vector, which makes the response more or less sensitive to individual phonons. A similar effect is seen in the relative strengths of the optic and acoustic contributions to the dynamic response function of simple ionic crystals in adjacent Brillouin zones. The spectra at F_c and F_d (figure 8) should in principle show the out-of-plane modes as well as the in-plane modes seen at F_a and F_b. The out-of-plane transverse acoustic mode at 97 cm^{-1} is clearly visible at F_c, though not at F_d, but the optic modes do not appear. On heating to 1125 K, a temperature at which there is a significant degree of orientational disorder, the situation becomes very different. All four spectra now have strong zero-frequency relaxational components and there are few signs of peaks that could be assigned to propagating modes. At 1200 K (not shown), where orientational disorder is complete, the responses at F_c and F_d are again centred at $\omega = 0$ but have smaller half widths than at 1125 K, while at F_a there is some evidence of a propagating mode at approximately 25 cm^{-1}. Inspection of the individual out-of-plane phonon spectra at 1200 K shows that there is a strong coupling between orientational and out-of-plane translational variables at all the accessible points along the line Γ–F, i.e. at (0, 0.125, 0.5), (0, 0.25, 1.5) and (0, 0.375, 1.5), and at the F point (0, 0.5, 2) itself. This coupling gives rise to a relaxational component at $\omega = 0$; indeed, except at the first of these points, the out-of-plane translational phonons are all overdamped. Even the in-plane translational phonons—those at (0, 0.125, 0.5), (0, 0.25, 1) and (0, 0.375, 1.5)—are influenced by the orientational disorder. All these spectra show a significant zero-frequency response, together with broadened phonon peaks, while at the F point (0, 0.5, 2) the in-plane transverse acoustic phonon has become overdamped and only a broad peak at approximately 100 cm^{-1} remains.

Diffuse scattering is strong at those values of q where fluctuations in $\rho(q)$ are large. As the phonons soften or acquire a relaxational character, there is a growth in the density fluctuations at the corresponding wavelengths. It follows that the enhancement with temperature of the diffuse scattering observed along line 2 (see figure 6) is associated with the increased sluggishness of the out-of-plane phonon response and the appearance of a relaxational component as the system disorders. A similar effect is seen in the low-frequency response of the in-plane phonons along Γ–F, but in that case it is most pronounced near the F point. Thus the growth in diffuse scattering with temperature is localized at the point F_a along line 1. The difference in $S(q)$ at F_a and F_b is related to the difference, already discussed, between the dynamic response functions at the same points. The dynamic response at F_a is dominated by the acoustic modes, while that at F_b also has a strong contribution from the optic modes. The latter, being of higher frequency, have a smaller amplitude and therefore contribute less to the diffuse scattering; they are also less affected by translation–rotation coupling. This explains why the diffuse scattering at F_b is weaker than that at F_a and why there is no significant temperature dependence associated with the scattering at F_b. Similarly, the more uniform behaviour and marked temperature dependence of $S(q)$ along line 2 is consistent with our observation that the out-of-plane

transverse acoustic phonon is strongly affected by translation–rotation coupling throughout the length of the line Γ–F rather than specifically at the F point.

3.5. Comparison with experiment

Dove *et al* [8] have reported the results of inelastic neutron-scattering measurements on the low-temperature phase of calcite at temperatures between 10 and 773 K. The experimental arrangement used did not provide the spectra at fixed q, but at cuts across the wavevector–energy plane. However, by following many paths, they were able to reconstruct the constant-q spectra; the q-values studied lie on our line 1 and include the points F_a and F_b. The reconstructed spectra have maxima in the range 30–40 cm^{-1}, corresponding to the in-plane transverse acoustic mode discussed in section 3.4, and a column of scattering extended from the phonon resonance down to zero frequency. As the temperature is raised, the mode softens, shifting by about 30 cm^{-1} from approximately 50 cm^{-1} at $T = 10$ K to an extrapolated value of approximately 20 cm^{-1} at 800 K. Simultaneously, the amplitude of the anomalous low-frequency scattering increases rapidly in a manner consistent with an Arrhenius-type relation. Although the q-vectors involved probe only the in-plane motion, the authors interpret their results as providing evidence for fluctuations into the monoclinic F^{1-} phase, implicitly by invoking the higher-order effects mentioned in section 3.2. In the simulation at 800 K, the low-frequency transverse acoustic mode at the F point occurs at 48 cm^{-1}, which represents a shift of only 7 cm^{-1} with respect to the frequency calculated [7] for the same potential model by harmonic lattice dynamics. Moreover, although the simulated F_a-point spectrum at 800 K does show some intensity at zero frequency, its amplitude relative to that of the phonon peak is much less than in the experimental spectrum. Hence the softening of the mode in the simulations and the associated growth in the low-frequency response are weaker than in the experiments. Closer to the transition the situation is more satisfactory. Unpublished constant-q measurements [14] of the temperature dependence of $S(q, \omega)$ at the point F_a show that at 1000 K the transverse acoustic mode is no longer visible and the recorded spectrum is qualitatively similar to the results obtained in the simulation at 1125 K. In other recent work, Harris [6] has described the results of a detailed study of the diffuse x-ray scattering from sodium nitrate near an F point that corresponds to point F_a of the present paper. He observed a strong temperature dependence similar to that seen in the simulation of calcite, as shown in figure 6(a). Harris [6] concludes that the experimentally observed scattering is associated not with fluctuations into another ordered structure but to the softening of the in-plane phonon modes of F^{2-} symmetry. As noted in section 3.2, the same effect could account for our own results for calcite.

4. Conclusions

We see from our calculations that the model proposed by Dove *et al* [10] provides an excellent description of certain features of the order–disorder transition in calcite, notably of the anomalous temperature dependence of the unit-cell parameters a and c and the behaviour of the order parameter η. It is less successful in reproducing details of the dynamic response function, at least at temperatures well below the transition. Despite these deficiencies, conclusions can be drawn that may have implications for the interpretation of experimental results. Wtihin the framework of the potential model used, there can be no doubt that F^{1-} ordering is less important than it is in comparable simulations of sodium nitrate. Nonetheless, the calculated diffuse scattering is strong and highly temperature dependent at the point F_a. Anomalous behaviour seen at F_a either in a neutron-scattering

experiment or in a simulation is therefore not necessarily indicative of an ordering instability at the F point of the type (F^{1-}) that has been envisaged. Clearly it would be worthwhile for new scattering experiments to be carried out at q-vectors that probe both the in-plane and out-of-plane motions of the ions.

Acknowledgments

We thank Dr M T Dove for helpful discussions and for communicating experimental results in advance of publication. The work has been supported in part by the United Kingdom SERC and by the CNR of Italy.

References

[1] Lynden-Bell R M, Ferrario M, McDonald I R and Salje E 1989 *J. Phys.: Condens. Matter* **1** 6523
[2] Schmahl W W and Salje E 1989 *Phys. Chem. Minerals* **16** 790
[3] Dove M T and Powell B M 1989 *Phys. Chem. Minerals* **16** 503
[4] Harris M J, Salje E and Guttler B K 1990 *J. Phys.: Condens. Matter* **2** 517
[5] Shinnaka Y 1964 *J. Phys. Soc. Japan* **19** 1281
[6] Harris M J 1993 *J. Phys.: Condens. Matter* **5** 5773
[7] Harris M J, Hagen M E and Dove M T 1992 unpublished
[8] Dove M T, Hagen M E, Harris M J, Powell B M, Steigenberger U and Winkler B 1992 *J. Phys.: Condens. Matter* **4** 2761
[9] Boyle L L and Kennedy J M 1988 *Z. Krystallogr.* **182** 39
[10] Dove M T, Winkler B, Leslie M, Harris M J and Salje E K H 1992 *Am. Mineral.* **77** 244
[11] Allen M P and Tildesley D J 1987 *Computer Simulation of Liquids* (Oxford: Oxford University Press)
[12] Dove M T, Swainson I P, Powell B M and Tennant D C 1993 unpublished
[13] Lynden-Bell R M, McDonald I R and Klein M L 1983 *Mol. Phys.* **48** 1093
[14] Dove M T 1993 private communication